24th COBEM - 2017

24th ABCM International Congress of Mechanical Engineering
December 3-8, 2017, Curitiba, PR, Brazil

COBEM-2017-0099
AERODYNAMIC DESIGN ANALYSIS OF A HYBRID VERTICAL WIND TURBINE FOR DECENTRALIZED POWER GENERATION

João Vicente Akwa
Engineering, Modeling and Applied Social Sciences Center, Federal University of ABC, Brazil
joao.akwa@ufabc.edu.br

Carlos Eduardo Guex Falcão
Mechanical Engineering Department, Federal University of Santa Maria, Brazil
cegfalcao@gmail.com

Abstract. *This work presents an aerodynamic analysis of a hybrid Darrieus/Savonius turbine. Performance characteristics and power curves of a pure Darrieus turbine are obtained by means of the Multiple Streamtubes Theory, which equals the forces on the aerodynamic profiles to the forces arising from the rate of change in flow momentum. To evaluate the performance in conjunction with the Savonius rotor, the torque and power curves obtained for the Darrieus turbine are combined with the classical curves of the chosen Savonius configuration, which are present in the literature. The method of operation of the hybrid turbine was obtained for dimensions suitable for microgeneration. This turbine presents a power coefficient of 0.49, slightly higher than the traditional Darrieus turbine, which presents a power coefficient of 0.43. Maximum efficiency occurs at 717.1 rpm considering a uniform airflow velocity of 10.75 m/s, which provides a mechanical power of 361.4 W.*

Keywords: *Darrieus turbine, Savonius turbine; hybrid turbine, multiple streamtubes*

1. INTRODUCTION

The study and understanding of wind turbines have been accomplished with success during the past century and Horizontal-axis wind turbines (HAWTs) are currently employed in large scale. The blades profiles are the most important feature generating lift for its operation. On another hand, Vertical-axis wind turbines (VAWTs) can have some advantages considering small-scale energy conversion in urban areas, on the top of buildings, roofs, and towers or close to the ground. In these turbines the lift generation mechanism is the same as in HAWTs, but it can easily work with winds from any direction and the electric generator or control systems can be installed in the tower, closer to the ground, easing the human access (Batista, *et al.*, 2015; Jin, *et al.*, 2015). However, at low tip speed ratios (TSR, with symbol λ), it can present very low – or even negative – torque, as explains Kirke (1998). Therefore, this low torque zone, also known as dead band, turns de start-up prohibitive. To overcome such limitation, one may suggest the combination of the previous turbine with another turbine that operates at lower λ in order to increase the band of operation, allowing the start-up at lower λ values. A Savonius turbine is an obvious option considering its characteristics and, also, it can be a low cost solution for a non-centralized or even for residential energy conversion. Figure 1 shows the hybrid turbine characteristics and its dimensions, which are well suited for microgeneration. To perform the aerodynamic analysis of the Darrieus turbine the model proposed by Strickland (1975), called Multiple Streamtubes Theory, is used. The model equals the forces on the aerodynamic profiles to the forces from the rate of change in flow momentum, making possible to obtain theoretical curves for power coefficient e mechanical power, providing a valuable tool to propose a new turbine concept. The procedure explained by Kirke (1998) is used for the analysis of the hybrid turbine, which consists in the summation of the Darrieus and Savonius turbines torques. For final conclusions matter, the overall performance of the hybrid turbine is taken into account based on the relation between the maximum power and the power supplied by the air flowing through the maximum area.

2. METHODOLOGY

2.1 Turbine parameters

Figures 1a and 1b show the turbine dimensions and configuration considered in this study. As already stated, the authors kept in mind the very small-scale energy exploration. The maximum diameter is 1 m and the height is 1 m as

well. The aerodynamic profile adopted is NACA-0018, which is widely used for Darrieus turbine designs. Drag and lift coefficients depending on the angle of attack can be found in Brusca, *et al*. (2014) and Sheldahl e Klimas (1981).

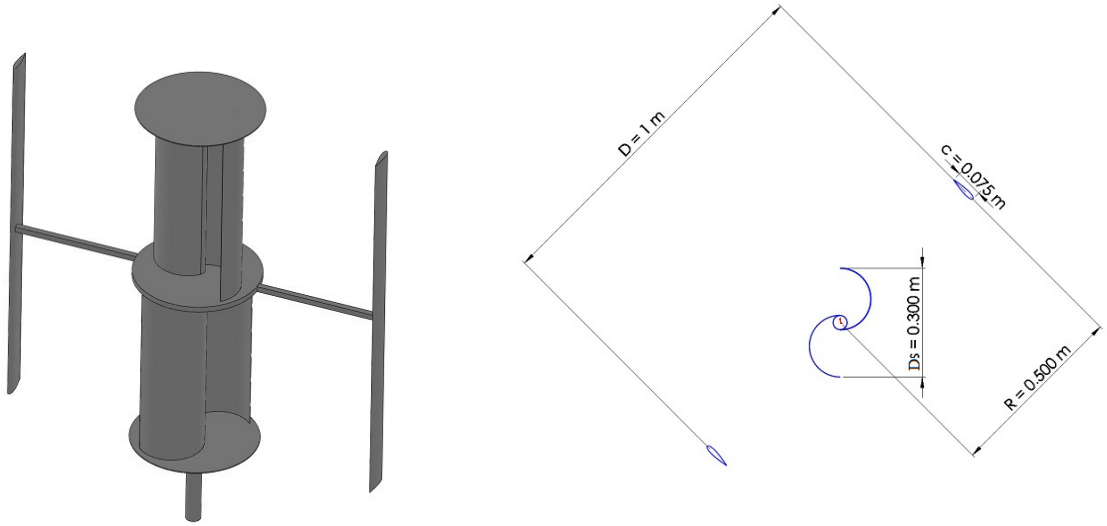

(a) (b)

Figure 1. VAWT: (a) Hybrid turbine 3D Plot (b) Important dimensions

Considering the Darrieus turbine, as analysed by Brusca, *et al*. (2014), the solidity σ should present values close to 0.3 in order to approach the maximum performance. Solidity σ is defined as the fraction of the control volume annular area which is covered by blades. Considering solidity definition showed by Eq. (1), adopting $\sigma = 0.3$ and $n_b = 2$, it is obtained a chord length of 0.075 m. In this equation n_b is the number of blades, c is the chord length and R is the maximum radius.

For the determination of the Savonius diameter coupled with the Darrieus turbine, the methodology explained by Kirke (1998) was adopted in order to establish a Savonius rotor with smaller diameter that will operate at same rotational speed than the Darrieus turbine but at lower λ, between 0 and 1.75, near to the lowest performance for Darrieus turbines, between 2 and 3. Therefore, it will be provided the sufficient torque for the start-up, decreasing the low or negative torque region of traditional Darrieus turbines. Considering λ the Tip Speed Ratio, ω the angular velocity and U_∞ the Wind velocity one can find the Savonius turbine radius of 0.3 m by Eq. (2). In addition, it is defined a two-stage turbine with no gap between buckets. Each stage of the Savonius rotor has 2 buckets and is rotated by 90° in relation to the adjacent stage. Between the stages are expected endplates with diameters equal to 1.1 times the diameter of the Savonius rotor. The remaining design strategies are in conformity with Akwa (2010) e Akwa, *et al.* (2012).

$$\sigma = \frac{n_b \cdot c}{R} \tag{1}$$

$$TSR = \lambda = \frac{\omega \cdot R}{U_\infty} \tag{2}$$

2.2 Multiple Streamtubes Theory

Figure 2 shows the general scheme of a Darrieus turbine. Lift and Drag coefficients can be found in the literature and can be used for estimation of torque and power. However, for a more precise calculation, one should consider the airflow over the aerodynamic profile, but the air decelerates as it passes through the turbine. The Multiple Streamtubes Theory is used to overcome such difficulty as it couples the aerofoil equations and rate of changing in flow momentum.

Using the Multiple Streamtubes Theory as proposed by Strickland (1975) for an H-rotor VAWT, the normal to the flow area should be divided in n streamtubes, each one having area A_s ($r \cdot \Delta\theta \cdot sen\theta \times \Delta h$), where r is the turbine radius,

θ the azimuthal angle and Δh the streamtubes height. The assumption $\Delta h = h$ is obvious since a small-scale wind turbine is considered and the velocity variation along the height is negligible.

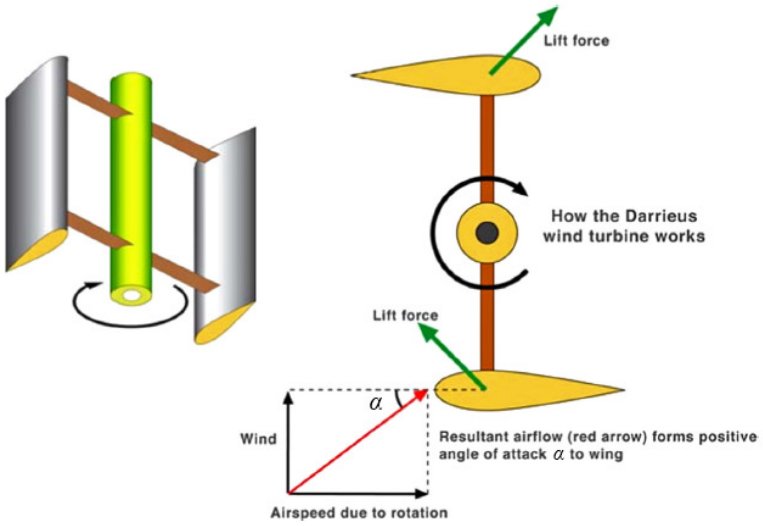

Figure 2. Darrieus turbine: General scheme and velocity vectors representation (Adapted from Jin, *et al*., 2015)

Solution considers eighteen streamtubes spaced 10 degrees, as shown in Fig. 3. Therefore, it becomes possible to obtain wind velocity quantities inside the blade acting regions. The use of spacing below 10 degrees does not show significant modification in the results.

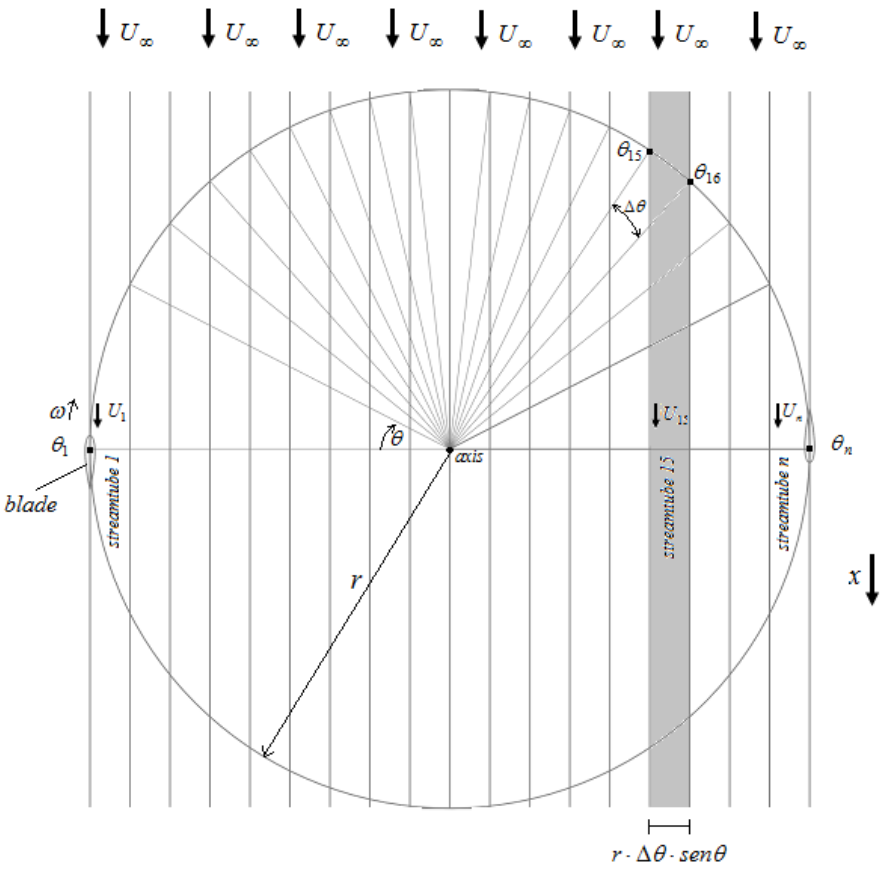

Figure 3. Streamtubes

The average force in the flow direction $\overline{F}_x$, considering the blade that passes through a determined streamtube, can be solved by

$$\overline{F}_x = 2 \cdot \rho \cdot A_s \cdot U\left(U_\infty - U\right) = 2 \cdot \rho \cdot \left(h \cdot r \cdot \Delta\theta \cdot sen\theta\right) \cdot U\left(U_\infty - U\right) \tag{3}$$

where ρ is the air density.

The percentage time spent by each blade element in a streamtube is $\Delta\theta/\pi$, therefore one can replace $\overline{F}_x$ by

$$\overline{F}_x = n_b \cdot F_x \cdot \frac{\Delta\theta}{\pi} \tag{4}$$

where F_x is the force considered over one single blade.

Combining as Equations (3) e (4) and multiplying by $1/U_\infty^2$:

$$\frac{n_b \cdot F_x}{2 \cdot \pi \cdot \rho \cdot r \cdot h \cdot sen\theta \cdot U_\infty^2} = \frac{U}{U_\infty} \cdot \left(1 - \frac{U}{U_\infty}\right) \tag{5}$$

For nomenclature and simplification matters, left hand side of the equation can be defined as F_x^*, yielding

$$F_x^* = \frac{n_b \cdot F_x}{2 \cdot \pi \cdot \rho \cdot r \cdot h \cdot sen\theta \cdot U_\infty^2} \tag{6}$$

It is possible to decompose F_x in tangential force F_t and normal force F_n, as shown in Fig. 4. Therefore, F_x is defined by Eq. (7).

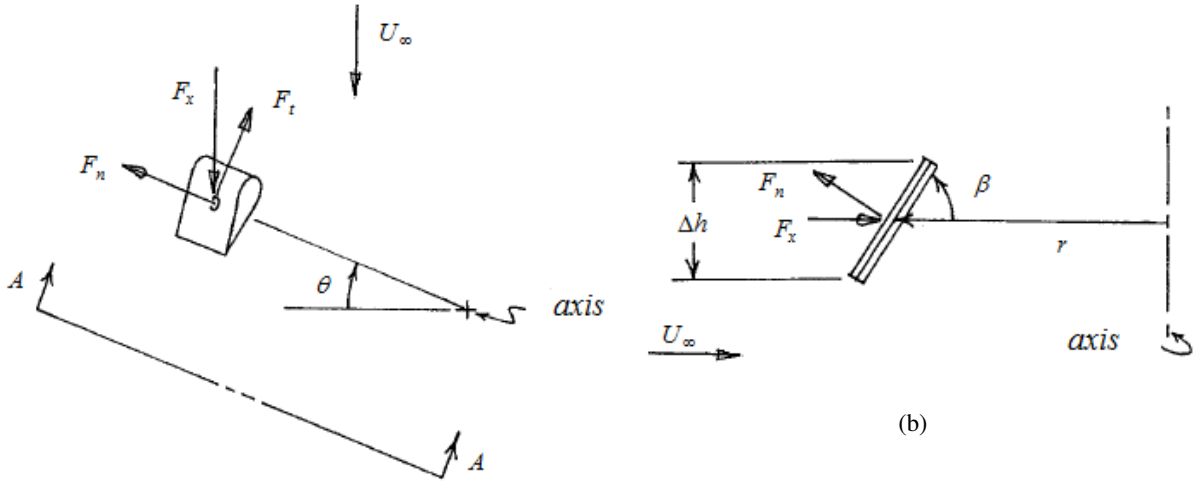

Figure 4. Forces on a blade: (a) plane view; (b) A-A view (Adapted from Strickland, 1975)

$$F_x = -\left[F_n \cdot sen\left(\pi/2\right) \cdot sen\theta + F_t \cdot \cos\theta\right] = -\left(F_n \cdot sen\theta + F_t \cdot \cos\theta\right) \tag{7}$$

F_t and F_n can be indirectly defined in terms of lift and drag coefficients, which are well known and easily found in the literature. In Eq. (8), U_R is the relative velocity and C_t and C_n are function of lift and drag coefficients, defined in Eq. (10).

$$F_t = \frac{1}{2} \cdot C_t \cdot \rho \cdot h \cdot c \cdot U_R^2 \tag{8-a}$$

$$F_n = \frac{1}{2} \cdot C_n \cdot \rho \cdot h \cdot c \cdot U_R^2 \tag{8-b}$$

Through nondimensionalization of Eq. (8) one obtains:

$$F_t^+ = \frac{F_t}{\frac{1}{2} \cdot \rho \cdot h \cdot c \cdot U_t^2} = C_t \cdot \left(\frac{U_R}{U_t} \right)^2 \tag{9-a}$$

$$F_n^+ = \frac{F_n}{\frac{1}{2} \cdot \rho \cdot h \cdot c \cdot U_t^2} = C_n \cdot \left(\frac{U_R}{U_t} \right)^2 \tag{9-b}$$

where U_t is the maximum tip tangential velocity.

C_t e C_n can be described based on the angle of attack α:

$$C_t = C_L \cdot sen\alpha - C_D \cdot \cos\alpha \tag{10-a}$$

$$C_n = C_L \cdot \cos\alpha + C_D \cdot sen\alpha \tag{10-b}$$

Combining Equations (6), (7) e (8), a new relation for F_x^* is encountered

$$F_x^* = \frac{n_b \cdot c}{4 \cdot \pi \cdot r} \cdot \left(\frac{U_R}{U_\infty} \right)^2 \cdot \left(C_n - C_t \cdot \frac{\cos\theta}{sen\theta} \right) \tag{11}$$

The angle of attack and the relative wind velocity are given by

$$tg\alpha = \frac{U \cdot sen\theta}{U \cdot \cos\theta + U_t} \tag{12}$$

$$U_R \cdot sen\alpha = U \cdot sen\theta \tag{13}$$

Using the classical definition of induction factor a (equals to $1 - U/U_\infty$) and the relations of Eq. (5) e (6), yields:

$$a = F_x^* + a^2 \tag{14}$$

As Strickland (1975) discusses, an analytical solution for F_x^* is prohibitive and an iterative solution should take place. Thus:

$$a_{new} = F_x^* + a_{old}^2 \tag{15}$$

The aforementioned equation is the core of Streamtubes Theory. The iterative process can be organized in 9 steps:

- 1: Initial guess: $a = 0$
- 2: to obtain α from Eq. (12)
- 3: to obtain C_t and C_n from Eq. (10) using C_L and C_D from aerodynamics profile charts

- 4: to obtain U_R from Eq. (13)
- 5: to obtain F_x^* from Eq. (11)
- 6: to update a with Eq. (15)
- 7: to obtain U from $a = (1 - U/U_\infty)$
- 8: to verify convergence criterion. If the criterion is reached, one must go to step 9, if not, go to step 2.
- 9: to calculate Darrieus turbine torque and power.

Average toque can be obtained from Eq. (16), where $n_{\Delta t}$ is the azimuthal angle number in increments of $\pi/n_{\Delta t}$.

$$\overline{T} = \frac{n_b}{n_{\Delta t}} \cdot \sum_{1}^{n_{\Delta t}} \left(\frac{1}{2} \cdot \rho \cdot r \cdot C_t \cdot c \cdot h \cdot U_R^2 \right) \tag{16}$$

Them it is possible to calculate the average power P and power coefficient C_P :

$$P = \overline{T} \cdot \omega \tag{17}$$

$$C_P = \frac{P}{P_{available}} = \frac{\overline{T} \cdot \omega}{\frac{1}{2} \cdot \rho \cdot (D \cdot h) \cdot U_\infty^3} = \frac{\overline{T}}{\frac{1}{2} \cdot \rho \cdot (D \cdot h) \cdot U_\infty^2 \cdot r} \cdot \frac{\omega \cdot r}{\cdot U_\infty} = C_T \cdot \lambda \tag{18}$$

Step 3 requires the update of C_D and C_L, performed through reading of tables or calculated from beforehand-interpolated functions. Generally this variables are functions of angle of attack and Reynolds number, and the latter, is defined as the Eq. (19) where μ is dynamic viscosity of air.

$$\mathrm{Re} = \frac{\rho \cdot U_t \cdot c}{\mu} = \frac{\rho \cdot \omega \cdot r \cdot c}{\mu} \tag{19}$$

3. RESULTS

In this chapter, results for power coefficient C_P vs. λ are shown and discussed. Comparing the present results to the results obtained by Brusca, *et al*. (2014) for an H-Darrieus two-bladed turbine (Fig. 5) with a solidity of 0.3 operating with a Reynolds number of 160,000 it is possible to verify that the methodology is precise and in conformity with previous works. In Figure 5, it is also possible to see dead band, characterized by low or negative torque, which implies in low efficiency in this TSR range.

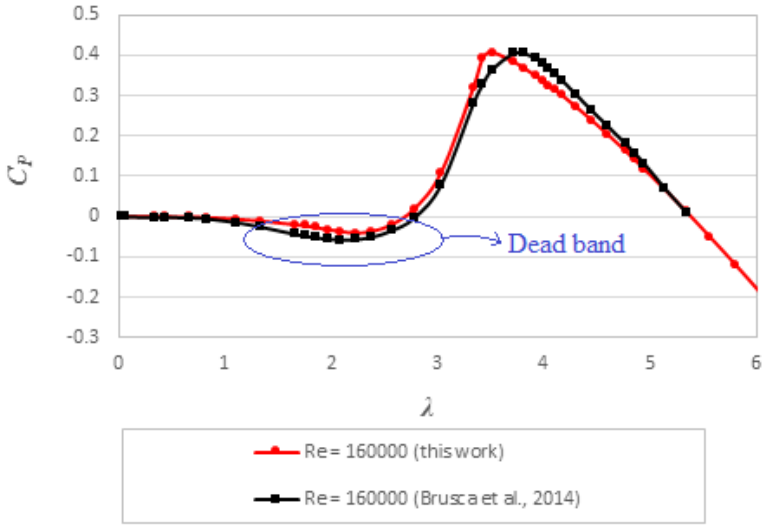

Figure 5. Power coefficient vs. λ.

It is possible to calculate power coefficient as Reynolds variation. If one considers the airflow velocity constant, turbine rotation will also vary in order to establish the required Reynolds. These results are shown in Figure 6 and 7. They show that power coefficient increases with rotational speed. As it happens, the dead band region gets narrower when Re increases improving considerably the start-up characteristics. The increase of power coefficient, obviously, is not linear and its value does not grow considerably between Reynolds numbers of 140,000 and 160,000, agreeing with Brusca, *et al.* (2014). For low rotational speeds, power coefficient can reach extreme negative values. This behaviour occurs because C_L grows and C_D decreases with Re increase, for flows below Re = 140,000, according the Fig. 8.

The method also allows obtaining the power curves for a Darrieus turbine working at different wind regimes, as Fig. 9 shows. The dark line shows a theoretical curve for best performance, that is, the line that links maximum power coefficient for each rotational speed. The other curves are for each wind velocity separately.

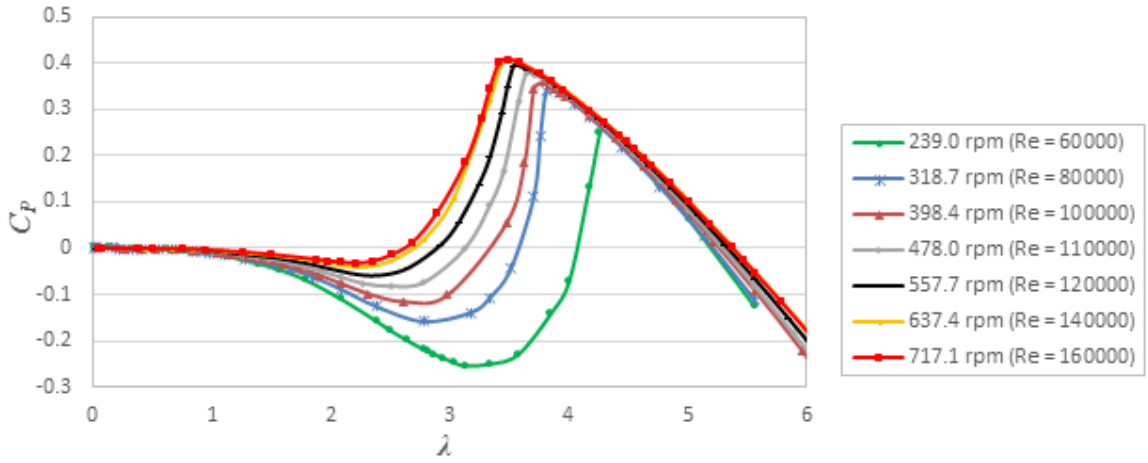

Figure 6. C_P *vs.* λ for Darrieus turbine.

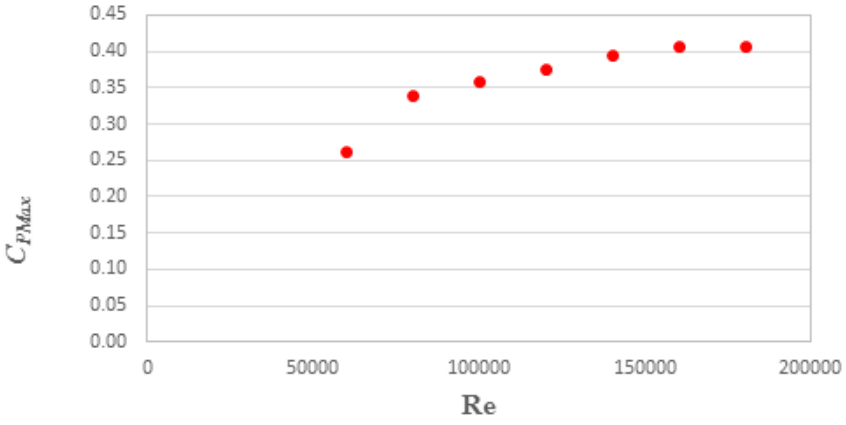

Figure 7. Maximum C_P vs. Re

Figure 8 shows lift and drag coefficients for the NACA 0018 profile for low attack angles. The values shown were used for the present calculations.

In order to decrease the dead band, it is possible to couple a Savonius rotor to the Darrieus turbine axis, as explained by Kirke (1998). Considering the Savonius rotor configuration studied by Blackwell, *et al.* (1978) it is possible to estimate values for power coefficient, as shown in Fig. 10a.

Observing the characteristics defined for both turbines, and the generated curves for its operational characteristics, Fig. 10b shows the power curves for the Darrieus turbine, Savonius turbine and the hybrid turbine for a wind speed of 8.25 m/s. The power for the hybrid turbine was generated by adding curves of each individual turbine, as explained by Kirke (1998). The result is an improved set, as shown in Fig. 11. The inclusion of Savonius turbine diminishes the dead band improving start-up characteristics. At lower rotational speeds, the hybrid turbine will have higher values of torque, and for consequence, higher power.

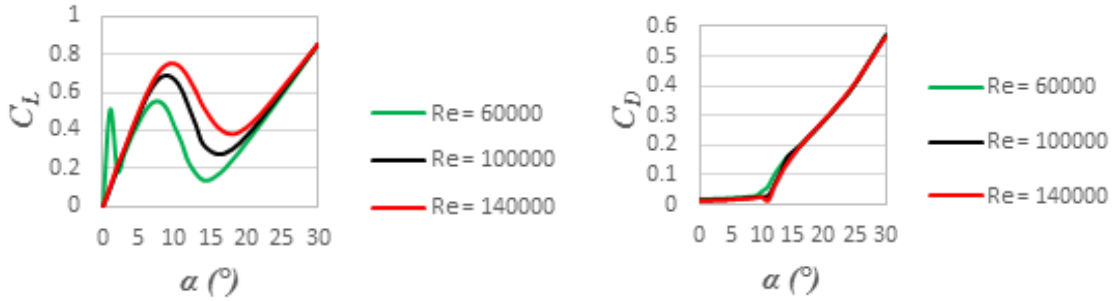

Figure 8. C_L e C_D vs. α for NACA-0018 (Sheldahl e Klimas, 1981)

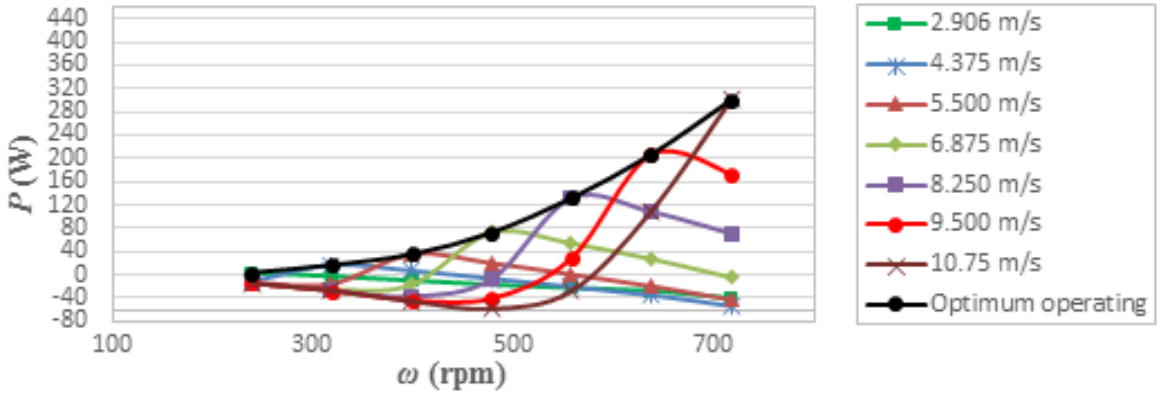

Figure 9. *P vs.* ω for Darrieus turbine.

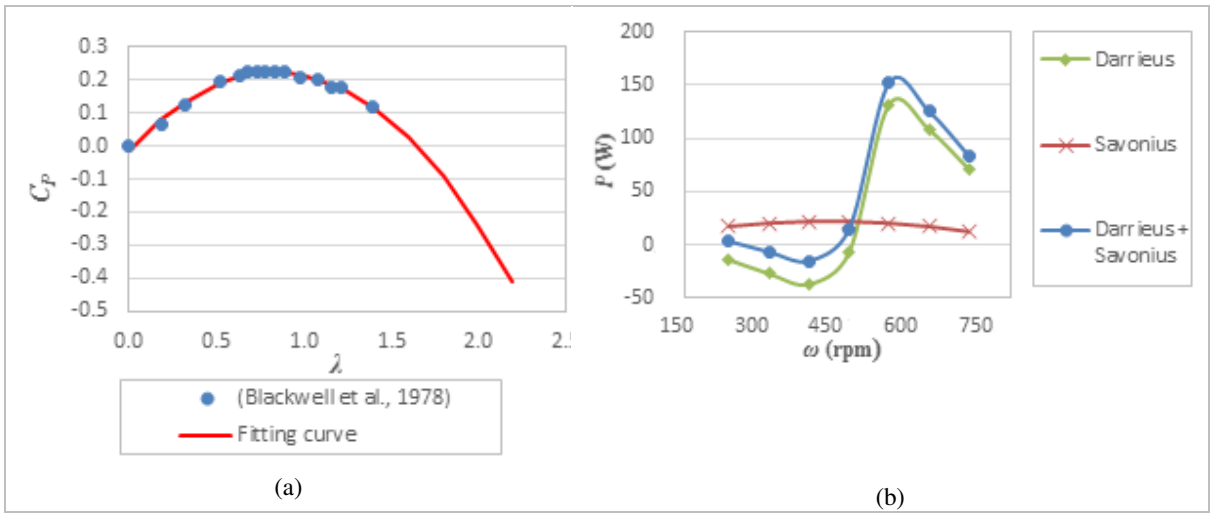

Figure 10. (a) C_P *vs.* λ for Savonius turbine; (b) three different concepts at wind speed of 8.25 m/s

With the addition of the Savonius rotor to the turbine axis, the dead band is narrower for all values of Re. This improves the start-up of the turbine because the torque of the device is positive for zero rotation. After starting the rotation, the turbine has its angular velocity increased by the beginning of the dead band. If the dead band is narrow, for any sudden reduction in wind speed (which occurs naturally in gusts of wind), the TSR value increases and the turbine re-accelerates to its optimum performance range. This occurs with horizontal turbines of low solidity, which have a narrow dead band. If the dead band is too large, the turbine cannot accelerate to TSR values above the lower limit of this band.

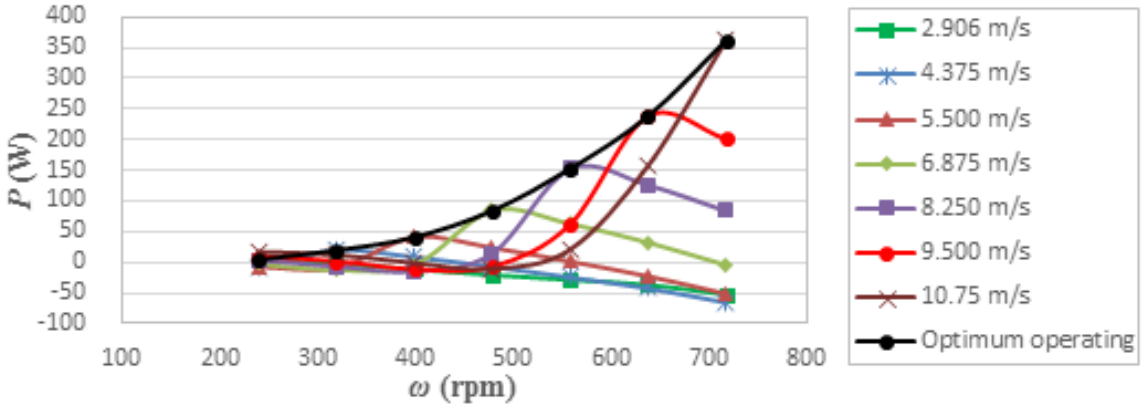

Figure 11. *P vs.* ω for the hybrid turbine (Darrieus + Savonius).

4. CONCLUSION

The present work studied different turbine concepts and discussed a hybrid concept aiming to reduce limitations of VAWTs for small-scale energy conversion. It applied the Multiple Streamtubes Theory and theoretically predicted power coefficient curves for the Darrieus turbine. It was shown the wide dead band region that prevents a satisfactorily start-up and diminishes the performance at lower rotational speeds. It was also shown its behaviour and the Reynolds number dependence along a range of rotational speeds.

In order to avoid start-up limitation, a Savonius turbine was coupled to the Darrieus turbine. Curves for the Savonius turbine were also acquired showing its better start-up characteristics. The hybrid turbine (Darrieus + Savonius) showed a maximum power coefficient of 49.3%, compared to 43.1% of Darrieus turbine alone. This point of maximum performance occurs for rotational speeds of 717.1 rpm considering a wind speed of 10.75 m/s, taken into account the dimensions and wind speeds adopted. The suggested turbine is a viable solution. It increases performance and power conversion for small-scale energy conversion not adding higher costs for its production.

5. REFERENCES

Akwa, J. V., 2010, "Análise Aerodinâmica de Turbinas Eólicas Savonius Empregando Dinâmica dos Fluidos Computacional", Universidade Federal do Rio Grande do Sul, Porto Alegre, Brasil, 128 p.

Akwa, J. V., Vielmo, H. A., Petry, A. P., 2012, "A review on the performance of Savonius wind turbines". Renewable and Sustainable Energy Reviews, Vol. 16, pp. 3054-3064.

Batista, N. C., Melício, R., Mendes, V. M. F., Calderón, M., Ramiro, A., 2015, "On a self-start Darrieus wind turbine: Blade design and field tests". Renewable and Sustainable Energy Reviews, Vol. 52, pp. 508-522.

Blackwell, B. F., Sheldahl, R. E., Feltz, L. V., 1977, "Wind Tunnel Performance Data for Two- and Three-Bucket Savonius Rotors", Final Report SAND76-0131, Sandia Laboratories, Albuquerque, USA, 105 p.

Brusca, S., Lanzafame, R., Messina, M., 2014, "Design of a vertical-axis wind turbine: how the aspect ratio affects the turbine's performance". Int. J. Energy Environ Eng., pp. 5:129.

Jin, X., Zhao, G., Gao, K., Ju, W., 2015, "Darrieus vertical axis wind turbine: Basic research methods". Renewable and Sustainable Energy Reviews, Vol. 42, pp. 212-225.

Kirke, B. K., 1998, "Evaluation of Self-starting Vertical Axis Wind Turbines for Stand-alone Applications", Griffith University, Gold Coast, Australia, 340 p.

Sheldahl, R. E., Klimas, P. C., 1981, "Aerodynamic Characteristics of Seven Symmetrical Airfoil Sections Through 180-Degree Angle of Attack for Use in Aerodynamic Analysis of Vertical Axis Wind Turbines", Energy Report, Sandia Laboratories, Albuquerque, USA, 120 p.

Strickland, J. H., 1975, "The Darrieus Turbine: A Performance Prediction Model Using Multiple Streamtubes", Energy Report, Sandia Laboratories, Lubbock, Texas, USA, 36 p.

6. RESPONSIBILITY NOTICE

The authors are the only responsible for the printed material included in this paper.